Neurobiology:

A Tyrosine-based Motif Localizes a Drosophila Vesicular Transporter to Synaptic Vesicles *in Vivo*

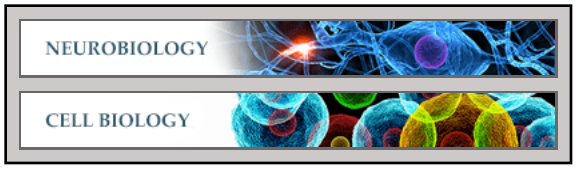

Anna Grygoruk, Hao Fei, Richard W. Daniels, Bradley R. Miller, Aaron DiAntonio and David E. Krantz

J. Biol. Chem. 2010, 285:6867-6878.
doi: 10.1074/jbc.M109.073064 originally published online January 6, 2010

THE JOURNAL OF BIOLOGICAL CHEMISTRY VOL. 285, NO. 10, pp. 6867–6878, March 5, 2010

A Tyrosine-based Motif Localizes a *Drosophila* Vesicular Transporter to Synaptic Vesicles *in Vivo*[*]

Received for publication, October 5, 2009, and in revised form, December 22, 2009 Published, JBC Papers in Press, January 6, 2010, DOI 10.1074/jbc.M109.073064

Anna Grygoruk[‡], Hao Fei[‡1], Richard W. Daniels[§1], Bradley R. Miller[§], Aaron DiAntonio[§], and David E. Krantz[‡2]

From the [‡]Department of Psychiatry and Biobehavioral Sciences, Semel Institute for Neuroscience and Human Behavior, Hatos Center for Neuropharmacology, David Geffen School of Medicine, UCLA, Los Angeles, California 90095-1761 and the [§]Department of Developmental Biology, Washington University School of Medicine, St. Louis, Missouri 63110-1093

Vesicular neurotransmitter transporters must localize to synaptic vesicles (SVs) to allow regulated neurotransmitter release at the synapse. However, the signals required to localize vesicular proteins to SVs *in vivo* remain unclear. To address this question we have tested the effects of mutating proposed trafficking domains in *Drosophila* orthologs of the vesicular monoamine and glutamate transporters, DVMAT-A and DVGLUT. We show that a tyrosine-based motif (Y*XX*Y) is important both for DVMAT-A internalization from the cell surface *in vitro*, and localization to SVs *in vivo*. In contrast, DVGLUT deletion mutants that lack a putative C-terminal trafficking domain show more modest defects in both internalization *in vitro* and trafficking to SVs *in vivo*. Our data show for the first time that mutation of a specific trafficking motif can disrupt localization to SVs *in vivo* and suggest possible differences in the sorting of VMATs *versus* VGLUTs to SVs at the synapse.

During synaptic vesicle (SV)[3] biogenesis, synaptic vesicle components traffic to the plasma membrane for assembly into mature synaptic vesicles (1, 2). In most current models, vesicles must undergo an internalization step at the plasma membrane to complete SV biogenesis. In addition, SV recycling requires endocytosis, and multiple modes of endocytosis may occur at the synapse (3). Genetic studies indicate that SVs cannot form in the absence of critical elements of the endocytic machinery (4–7). It remains surprisingly unclear, however, how particular trafficking motifs sort proteins to SVs. Although it is thought that endocytic motifs in vesicular proteins such as vesicular neurotransmitter transporters are likely to be required for their localization to SVs (8), this critical idea has never been explicitly tested in an intact animal. Moreover, it remains unclear whether all vesicular proteins use the same trafficking motifs and pathways to sort to SVs. Here, we have begun to investigate these questions in *Drosophila* using two structurally divergent vesicular neurotransmitter transporters.

Vesicular transporters are required for the transport of neurotransmitter into the lumen of SVs and include specific transporters for acetylcholine (9), γ-aminobutyric acid and glycine (10, 11), glutamate (12), and monoamines (9). *In vitro* trafficking studies of the neural isoform of mammalian VMAT (VMAT2) have shown that an Ile-Leu (dileucine) sequence within the cytoplasmic C terminus is necessary for endocytosis in PC12 cells and hippocampal neurons (13, 14) and localization to synaptic-like microvesicles (SLMVs) in PC12 cells (15). A dileucine and possibly an additional tyrosine-based motif in rat VAChT allows internalization from the cell surface and localization to SLMVs in neuroendocrine cells (16–18). A variant of the dileucine motif (FV) as well as a polyproline motif have been proposed to allow internalization of VGLUT1 and recycling to SVs in cultured neurons (19–21).

Although much is known about the function of transporter trafficking motifs *in vitro*, the role of specific motifs for the trafficking of SV proteins *in vivo* has not been investigated. *In vivo* models of transporter trafficking will be essential to understand its impact on neurotransmission and behavior. To address this issue, we are using the model genetic organism *Drosophila melanogaster.* Our groups have previously identified the *Drosophila* ortholog of VGLUT (DVGLUT) (22) and two splice variants of *Drosophila* VMAT, DVMAT-A and DVMAT-B, that differ at their C terminus (23). We have determined that DVGLUT and DVMAT-A are expressed in all glutamatergic and aminergic neurons, respectively (23–27). Here we show that a tyrosine-based motif in DVMAT-A is necessary for internalization in cultured cells *in vitro*. Importantly, mutation of this site dramatically reduces the localization of DVMAT-A to SVs *in vivo*. In contrast, we find that deletion of the entire presumptive trafficking domain in DVGLUT minimally affects internalization *in vitro*, or sorting to SVs *in vivo*. These studies demonstrate for the first time the importance of a trafficking motif for sorting VMATs or any other vesicular protein to SVs *in vivo*. Our data also suggest possible differ-

* This work was supported, in whole or in part, by National Institute of Mental Health Grant MH076900, National Institutes of Health Grants ES015747 (to D. E. K.) and ES016732 (to M. F. Chesselet) from NIEHS, National Institute on Drug Abuse Grant DA020812, and National Institutes of Health Grant NS051453 from NIDDK (to A. D.). This work was also supported by UCLA Molecular and Cellular and Neurobiology Training Grant T32MH019384 and the Achievement Reward for College Scientists Foundation (to A. G.).

[1] Both authors contributed equally to this work.

[2] To whom correspondence should be addressed: The Gonda (Goldschmied) Neuroscience and Genetics Research Center, 695 S. Charles E. Young Drive, Los Angeles, CA 90095-1761. Tel.: 310-206-8508; Fax: 310-206-9877; E-mail: dkrantz@ucla.edu.

[3] The abbreviations used are: SV, synaptic vesicle; VMAT, vesicular monoamine transporter; PC, pheochromocytoma cell; SLMV, synaptic-like microvesicle; VAChT, vesicular acetylcholine transporter; VGLUT, vesicular glutamate transporter; DCSP, *Drosophila* cysteine string protein; S2, Schneider line 2; HA, hemagglutinin; GFP, green fluorescent protein; LDCV, large dense core vesicle; LI, dileucine; Δ, deletion; mAb, monoclonal antibody; PBS, phosphate-buffered saline; FBS, fetal bovine serum; ANOVA, analysis of variance.

ences in the trafficking of VMATs *versus* VGLUTs at the synapse.

EXPERIMENTAL PROCEDURES

Fly Stocks—Flies were raised on corn meal-molasses agar media at 23–25 °C and 20–40% humidity in a 12-h light/dark cycle. Genetic crosses were performed according to standard procedures (28).

Site-directed Mutagenesis—To generate the *dVMAT-A* deletion mutants, Δ1, Δ2, and Δ3, the PCR was used to amplify a segment of a previously generated *pMT-dVMAT-A* construct (23) using a 30-bp oligonucleotide containing an internal stop codon and a distal XbaI site. Similarly, PCR-mediated site-directed mutagenesis was used to convert individual codons to alanine and generate Y600A, Y603A, Y606A, LI589/590AA, Y600/603A, and Y603/606A. Bulky group substitutions Y600F, Y600L, Y603F, and Y603L were also generated using PCR. The PCR products were digested with XbaI and RsrII in the *dVMAT* cDNA and inserted into *pMT-dVMAT-A*(*wt*) (23) and *pEx-UAS-dVMAT-A*(*wt*) (26) for expression in cultured *Drosophila* cells and in flies, respectively. All inserts were fully sequenced (UCLA DNA Sequencing Core, Los Angeles, CA). To generate the N- and C-terminal deletions of *dVGLUT* we used PCR and flanking primers to, respectively, introduce a new start codon at position 92 in the N terminus or a stop codon after Val^{529} in the C terminus of *dVGLUT* ($Trp^{530} \rightarrow$ Stop).

Cell Culture—Drosophila Schneider Line 2 (S2) and *Drosophila* DmBG2C6 cells (*Drosophila* Genomics Resource Center, Bloomington, IN) were grown at 25 °C in room air using Schneider's media (Invitrogen) containing 10% calf serum and 1% penicillin/streptomycin. Both S2 and *Drosophila* DmBG2C6 cells were transfected using FuGENE (Roche Applied Science) as per the manufacturer's instructions. For expression of cDNAs using the metallothionein promoter encoded in the vector pMT (Invitrogen), cells were incubated in 0.7 mM copper sulfate (CuS) for 24 h prior to endocytosis assays.

Endocytosis Assays—Internalization assays for wt and mutant DVMAT-A and DVGLUT were performed using a previously described assay (13, 23). Cells were plated on poly-D-lysine-covered coverslips in 24-well plates and transiently transfected with cDNAs representing either wt or mutant *dVMAT-A* or *dVGLUT*. One day following induction with 0.7 mM CuS, live S2, or *Drosophila* DmBG2C6 cells were incubated over ice for 1 h in 1:250 HA.11 mAb (Covance Research Products, Denver, CO), which recognizes the HA tag inserted in the lumenal loop common to all DVMAT-A constructs (23). For endocytosis studies of DVGLUT, we employed a *myc*-tagged construct (site 1 in Ref. 29) and 1:400 mAb 9E10 (Santa Cruz Biotechnology, Santa Cruz, CA). Following incubation with either HA.11 or 9E10, cells were either fixed immediately for 20 min in 4% paraformaldehyde, 0.1 M NaP_i, pH 7.4, or incubated at room temperature (23 °C) for 5–30 min prior to fixation to allow internalization of transporter that had been labeled at the cell surface. Following six washes in 1× PBS and permeabilization using 1× PBS containing 0.2% Triton X-100 and 5% fetal bovine serum (PBST/FBS), cells were incubated in 1:1000 anti-mouse secondary antibody conjugated to Cy3 (Jackson ImmunoReasearch Laboratories, West Grove, PA) for 45 min. Cells were then washed three times in PBST/FBS, rinsed once in 1× PBS, mounted using Prolong Antifade (Molecular Probes, Eugene, OR), and visualized using a Zeiss LSM 5 Pascal confocal microscope. Either a 63× or a 100× Neofluar objective was used for quantitation of pixel intensity *versus* high resolution images, respectively. For quantitation, images of individual cells were manually divided into total and internal regions (see Fig. 2*B*). Measurements of the mean pixel intensity and area of each region were obtained using Zeiss LSM 5 Pascal software. To measure surface/perimembranous pixels, areas both outside of the cell (beyond the "total" boundary) and within the "internal" boundary were masked (shown as *gray* in Fig. 2*B*), and the pixels within the resulting region were quantitated. To normalize for cell-to-cell variation in expression, pixel intensities in the internal and surface regions were expressed as a ratio of total cellular intensity using Equations 1 and 2.

$$\frac{\text{Internal}}{\text{Total}} = \frac{[\text{internal mean pixel intensity} \times \text{internal area } (\mu m^2)]}{[\text{total mean pixel intensity} \times \text{total area } (\mu m^2)]} \quad \text{(Eq. 1)}$$

$$\frac{\text{Surface}}{\text{Total}} = \frac{[\text{surface mean pixel intensity} \times \text{surface area } (\mu m^2)]}{[\text{total mean pixel intensity} \times \text{total area } (\mu m^2)]} \quad \text{(Eq. 2)}$$

dVMAT-A Transgenic Fly Lines—To create *Y600A dVMAT-A* transgenic flies, *pEx-UAS-Y600A-dVMAT-A* was co-injected with the *pΔ2–3* plasmid, a source of transposase, into ~500 *yw* embryos using standard methods (30). Lines containing *pEx-UAS-Δ3-dVMAT-A* and *pEx-UAS-Δ2-dVMAT-A* were generated by Rainbow Transgenic Flies Inc. (Newbury Park, CA). The wt line containing *pEx-UAS-dVMAT-A* on the second chromosome has been previously reported (26). *Elav-GAL4* was used to express all *dVMAT*-A transgenes. The following lines were used for glycerol velocity gradient fractionation experiments: *elav-GAL4(x)/+;UAS-DVMAT-A(II)/+;elav-GAL4(III)/+* (*WT* in Fig. 6), *elav-GAL4(III),UAS-Y600A(III)/elav-GAL4 (III),UAS-Y600A(III)* (*Y600A* in Fig. 6), *elav-GAL4(III),UAS-Δ2(III)/elav-GAL4(III),UAS-Δ2(III)* (*Δ2* in Fig. 6), and *elav-GAL4(III),UAS-Δ3(III)/elav-GAL4(III),UAS-Δ3(III)* (*Δ3* in Fig. 6).

dVGLUT Mutagenesis—Male flies homozygous for the *UAS-GFP-dVGLUT* transgene on chromosome II (24) were fed a solution of 5% sucrose and 22 mM methanesulfonic acid ethyl ester (Sigma) for 12–16 h and then mated to virgin *dVGLUT-GAL4* (on the X chromosome) females at 25 °C. The progeny of this cross (*dVGLUT-GAL4(x);UAS-GFP-dVGLUT(II)/+*) generally die as pupae due to overexpression of DVGLUT; rare escapers eclose, but their wings fail to inflate. To screen for suppressors, we selected progeny that 1) eclosed and 2) had clearly inflated wings. These adults were crossed to *w; Sco/CyO* to propagate suppressor mutations on the second chromosome. To determine whether suppressor mutations were indeed on chromosome II, male progeny (*w; CyO/potentially mutagenized chromosome II*) were backcrossed to *dVGLUT-GAL4(x)* virgins. Mutagenized chromosomes containing the suppressor mutations were maintained over *CyO* in a *w* back-

ground. Genomic DNA was isolated from suppressor lines and used as template for PCR to amplify the *UAS-GFP-dVGLUT* transgene. The transgene was sequenced using standard methods at the Protein and Nucleic Acid Chemistry Laboratories at Washington University, St. Louis. The B3 line (see Table 1, row 39) is also designated as *UAS-GFP-dVGLUT-ΔC* under "Results and Discussion."

Western Blots—For Western blots comparing total *dVMAT-A* transgene expression in wt and mutant fly lines, flies were aged 3–4 days, anesthetized using CO_2, and either 6 or 7 heads per genotype were homogenized in buffer containing 10 mM Tris-HCl, pH 7.4, 0.8 M NaCl, 1 mM EGTA, pH 8.0, 10% sucrose and proteinase inhibitor mixture (Roche Applied Science). Protein assays (Bio-Rad Laboratories, Hercules, CA) were performed on each homogenate, and samples were loaded onto an acrylamide gel, followed by transfer to nitrocellulose. Membranes were incubated overnight at 4 °C with primary antibodies, including mouse anti-HA.11 (1:1000) to detect DVMAT-A, and mouse anti-β-tubulin (1:4000, Developmental Studies Hybridoma Bank, Iowa City, IA) as a loading control. For Western blot analysis of glycerol gradient fractionation, additional primary antibodies included an mAb directed against *Drosophila* cysteine string protein (DCSP, 1:2000, Developmental Studies Hybridoma Bank), which served as a marker for SVs (31, 32), rabbit anti-DVGLUT (1:5000) and rabbit anti-GFP (1:1000, Invitrogen, A-11122). All blots were then probed with either anti-mouse or anti-rabbit horseradish peroxidase-conjugated secondary antibodies (1:1000 to 1:2000, Amersham Biosciences) for 45 min at ambient temperature, followed by SuperSignal West Pico Luminol/Peroxide (Pierce), and exposed to Kodak Biomax Light Film (Rochester, NY). Care was taken to avoid saturation. Images were digitized and quantified using ImageJ (National Institutes of Health freeware). Statistical analysis was performed using GraphPad Prism (San Diego, CA).

Glycerol Gradient Fractionation—Flies were frozen on dry ice, and heads were separated from bodies using wire mesh sieves. Heads were ground on dry ice using a mortar and pestle and homogenized using Teflon on glass in ice-cold homogenization buffer containing 10 mM HEPES, 1 mM EGTA, 0.1 mM $MgCl_2$ (pH = 7.4) and a protease inhibitor mixture (Roche Applied Science). The homogenate was centrifuged for 2 min at 1000 × *g*, 4 °C, and the postnuclear supernatant was layered onto a 5–25% glycerol gradient over a 50% sucrose pad. Gradients were centrifuged for 1 h and 15 min, 4 °C at 40,400 rpm in a Beckman SW41 rotor; 16–17 fractions were subsequently collected from the bottom and analyzed by Western blot analysis (see above). In addition to the gradient fractions, samples of the postnuclear supernatant were diluted 10-fold and analyzed in parallel on the same blot (input or "*i*" in Fig. 6*C*). Dilution of the postnuclear supernatant was performed to prevent overexposure of the input signal during later chemiluminescent analysis of the blots. Several input samples (representing 1–5 μl of postnuclear supernatant input) were loaded in parallel to ensure that at least one would later generate a digitized signal in the linear range for quantitation. To simplify Fig. 6*C*, only one of the input lanes is shown for each gradient. For each immunoblot, the x-ray films representing the chemiluminescence signals from the input lanes and the gradient fractions containing SVs (the DCSP peak) were digitized and quantified for pixel intensity (ImageJ, NIH). (The *bands* in *lanes 1* and *2* at the bottom of the gradient were not quantitated and not used for further calculations). One of the input lanes found to be in the linear range of the digitized output was selected for further calculations. The amounts of HA-tagged DVMAT-A and DCSP in the SV fractions (those containing the DCSP peak) were expressed as a percentage of the immunoreactivity contained in the selected input lane (see formula below). To correct for potential experimental differences between each gradient, anti-HA immunoreactivity representing DVMAT-A was normalized to anti-DCSP immunoreactivity in the quantified SV fractions using the formula,

$$\frac{(\text{DVMAT in DCSP peak fractions}/\text{DVMAT input})}{(\text{DCSP in peak fractions}/\text{DCSP input})} = \text{DVMAT on SVs} \quad \text{(Eq. 3)}$$

where

$$\text{"Input"} = \frac{(\text{immunoreactivity in input lane})}{(\text{dilution factor for input lane})} \times (\text{volume loaded on gel}). \quad \text{(Eq. 4)}$$

To calculate the relative amounts of endogenous DVGLUT and the GFP-DVGLUT-ΔC fusion on SVs, a similar method was used. Vesicular DVGLUT was normalized to total DVGLUT, and vesicular GFP-DVGLUT-ΔC was normalized to total GFP-DVGLUT-ΔC. The two numbers were directly compared and calculated for a difference in percentage. Serial dilutions from each relevant fraction were quantified to improve precision.

RESULTS

Deletion Mutants of DVMAT-A Show Internalization Deficits in Vitro—Similar to mammalian vesicular transporters, *DVMAT-A* readily internalizes from the plasma membrane *in vitro* (23). Sequence analysis of the *dVMAT-A* cDNA identified several predicted amino acids similar to those shown to be important for trafficking of rat VMAT2 (Fig. 1*A*). To determine which amino acids within the C terminus of DVMAT-A are necessary for internalization, we used site-directed mutagenesis to generate a series of C-terminal truncations (Fig. 1*A*). These include: Δ3, which includes a potential dileucine motif and all distal residues; Δ2, which includes potential tyrosine-based signals; and Δ1, which deletes four acidic residues that form a possible acidic patch motif (33) (Fig. 1*A*). To test the deletion mutants' ability to internalize from the cell surface, we transiently expressed them in *Drosophila* S2 cells and employed a previously described endocytosis assay (13, 23). The lumenal domain of DVMAT-A is transiently exposed to the extracellular milieu when vesicles fuse with the plasma membrane. The internalization of antibodies directed against a lumenal HA tag therefore provides a convenient method to visualize endocytosis. Similar to our previously reported data (23), we found that wild-type (wt) DVMAT-A appeared to be completely internalized within 30 min at 23 °C (Fig. 2*A*). In contrast, both the Δ3

FIGURE 1. **DVMAT-A and DVGLUT C-terminal mutants.** The distal end of the last transmembrane domain and terminal residues are respectively indicated with *gray bars* and *gray numbers*. *A*, the cytoplasmic C termini of rat VMAT2 and DVMAT-A. *Boxed residues* in VMAT2 indicate trafficking motifs, including a dileucine motif with upstream acidic residues (KEEKMAIL) and downstream acidic patch (DDEESESD). For DVMAT-A, we indicate the extent of three deletions (Δ1–3) and the position of point mutants, including tyrosines 600, 603, and 606 (*white text*, *black background*) and a potential dileucine motif at 589/590 (*black text*, *gray background*). *B*, the C terminus of DVGLUT and rat VGLUT1 are shown. *Boxed residues* in VGLUT1 (SEEKCGFV) indicate a proposed dileucine-like motif present in VGLUT1, -2, and -3 (19). A second signal (*underlined PPRPPPP*) is present in VGLUT1 but not VGLUT2 or -3. For DVGLUT, the site of mutations identified in the suppressor screen are indicated (see also Table 1). Tyrosines (*white text*, *black background*) and a pair of hydrophobic residues in DVGLUT (*gray background*) are highlighted as potential endocytosis motifs.

and Δ2 mutants were retained on the cell surface (Fig. 2*A*). The Δ1 mutant did not have a detectable effect on internalization (data not shown). To quantitate these observations, we measured pixel intensity of signal at or near the cell surface *versus* signal in the interior of the cell (see "Experimental Procedures" and Fig. 2*B*). Both values were normalized to total DVMAT-A labeling in each cell. We found that after 30 min, 82% of DVMAT-A wt was internalized, whereas only 36% of Δ3 and 42% of Δ2 were internalized from the plasma membrane (Fig. 2*C*, one-way ANOVA, $p < 0.0001$; *three asterisks* represent Bonferroni post test, $p < 0.001$ as indicated).

Because the Δ2 and Δ3 deletions had similar effects on endocytosis, our data suggest that the primary endocytosis signal for DVMAT-A is contained within the Δ2 deletion. However, because the Δ3 mutant internalized slightly less than Δ2 (Bonferroni post test, $p < 0.001$), it remains possible that additional motifs upstream of Δ2 could contribute to DVMAT-A endocytosis.

The C Terminus of DVMAT-A Contains a Tyrosine-based Motif Necessary for Efficient Endocytosis in S2 Cells—Multiple studies have shown that tyrosine-based motifs can function as endocytosis signals (for review see Ref. 34). To determine which tyrosine(s) contained within the Δ2 region of DVMAT-A might mediate DVMAT-A's internalization from the cell surface, we made single point mutations of each residue (Y600A, Y603A, and Y606A) as well as the combined mutations Y600/603A and Y603/606A (see Fig. 1*A*). Because Δ3 contains a potential dileucine motif ($LI^{589/590}$) similar to VMAT2 and showed a slightly more severe endocytosis defect than Δ2, we also mutated these residues (Fig. 1*A*). We found that the Y606A and the dileucine (LI589/590AA) mutants were efficiently endocytosed (77 and 74%, respectively) within 30 min at 23 °C (Fig. 3, *A* and *B*), although there was a slight difference between these two mutants and DVMAT-A wt (see Fig. 3). In contrast, only 39% of Y600A internalized from the cell surface (ANOVA, $p < 0.0001$; Bonferroni post test, $p < 0.001$ between wt and Y600A). Mutating Tyr^{603} had a similar, but lesser effect; 45% was internalized (Bonferroni post test, $p < 0.001$ between wt and Y603A). The double mutant Y600/603A, and to a lesser extent Y603/606A, showed a defect in endocytosis similar to Y600A (not shown). These findings strongly suggest that the $^{600}YXXY^{603}$ motif in the C terminus of DVMAT-A is a major determinant of endocytosis. Furthermore, unlike mammalian VMAT2 and VAChT, the putative dileucine motif in DVMAT-A may not function as the primary endocytosis signal.

YXXY May Be a Variant of the Known YXXΦ Motif—The initial tyrosine residue in the canonical tyrosine-based motif YXXΦ (where Φ represents a bulky hydrophobic residue) is essential for its function, and in most cases cannot be replaced by other hydrophobic or aromatic amino acid residues; in contrast, the requirements at the last position are less stringent (35). To determine whether the $^{600}YXXY^{603}$ motif in the C terminus of DVMAT-A is a novel motif, or a variant of YXXΦ, we separately substituted Tyr^{600} and Tyr^{603} with either phenylalanine or leucine residues and performed internalization assays as described above. Similar to the Y600A mutant, only 45% of Y600F and 43% of Y600L internalized from the cell surface (Fig. 4, *A* and *B*). In contrast, both Y603F and Y603L mutants internalized similarly to DVMAT-A wt (Fig. 4, *A* and *B*). These data show that the tyrosine in the second, but not the first position in the $^{600}YXXY^{603}$ motif can be substituted by a bulky residue and suggest that $^{600}YXXY^{603}$ may be a variant of the YXXΦ motif (see "Discussion").

Endocytosis in a Neuronal Cell Line—Neuronal and non-neuronal cells differ in many respects, and at least some trafficking events, such as calcium-mediated exocytosis, are relatively specific for neurons and endocrine cells. Similarly, some cell types may favor particular endocytic pathways, although this remains poorly understood. Because S2 cells are not neuronal and DVMAT-A is endogenously expressed in neurons (23, 26), we tested DVMAT-A endocytosis in the *Drosophila* cell line DmBG2C6, which expresses the neuronal markers horseradish peroxidase and the neuropeptides substance P, proctolin, and somatostatin (36). The dopamine precursor L-3,4-dihydroxyphenylalanine (L-DOPA) and low levels of acetylcholine have also been detected (36, 37). DVMAT-A wt was efficiently endocytosed in *Drosophila* DmBG2C6 cells, whereas DVMAT-A Δ3, Δ2, and Y600A remained largely at the cell surface (Fig. 5). These results support the idea that the

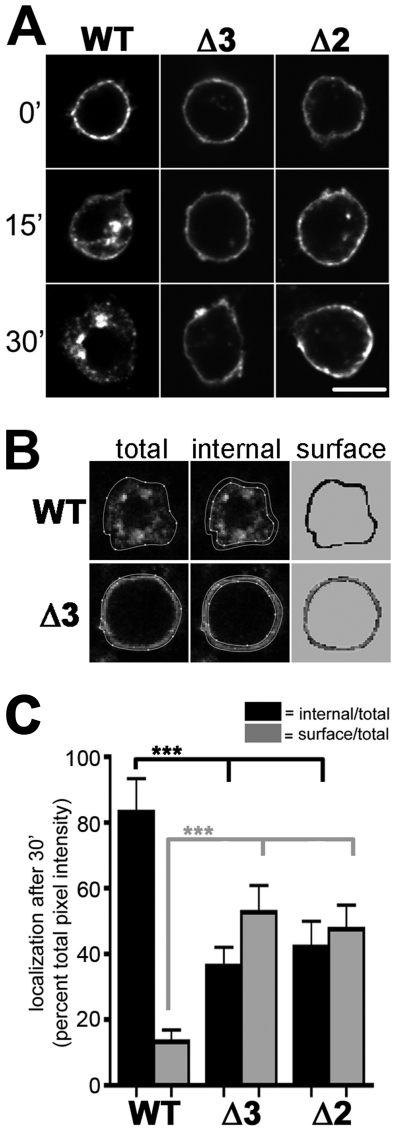

FIGURE 2. **Endocytosis of DVMAT-A deletion mutants in cultured *Drosophila* S2 cells.** *A*, S2 cells transiently transfected with *dVMAT-A* wt, Δ3, or Δ2 constructs were incubated in HA antibody for 1 h on ice. Cells were then either fixed immediately on ice (*0′*), or incubated for 15 min (*15′*) or 30 min (*30′*) at 23 °C to allow endocytosis. Wild-type DVMAT-A (*wt*) was largely internalized following 30-min incubation, whereas both the Δ3 and Δ2 mutants remained on the cell surface. *Scale bar*, 5 μm. *B*, to quantitate internalization, cells were manually divided into total and internal regions. These are shown enclosed by *dotted white lines* in representative examples of wt and Δ3 cells (*left* and *middle panels* as indicated). The surface/perimembranous region (*right hand panels*), was obtained by digitally masking (shown in *gray*) both the area outside of the cell (outside the "total" boundary) and the area within the "internal" boundary. Pixels within the remaining ring were then quantified as "surface." To normalize for cell-to-cell variation in total cellular expression, the pixel intensity in the surface and internal regions was expressed as a ratio of either internal/total or surface/total intensity respectively (see "Experimental Procedures" for equations). Note that images used for quantitation in *B* were obtained at lower magnification than those shown in *A* and therefore appear more pixilated. *C*, quantitation of pixel intensity at the 30-min time point for internalized (*black columns*) and cell surface immunoreactivity (*gray columns*), both normalized for total immunoreactivity per cell. For DVMAT-A wt, 82.2 ± 4.7% was internalized (mean ± S.D., ≥77 cells from ≥3 separate experiments for each genotype). In contrast, 36.3 ± 5.9% of DVMAT-A Δ3 and 42.1 ± 7.8% of DVMAT-A Δ2 internalized. One-way ANOVA, $p < 0.0001$, with Bonferroni post test, $p < 0.001$ (*black asterisks*) between internal wt and both Δ2 and Δ3; one-way ANOVA, $p < 0.0001$, with Bonferroni post test, $p < 0.001$ (*gray asterisks*) between cell surface wt and both Δ2 and Δ3.

^{600}YXXY^{603} motif is important for DVMAT-A endocytosis in both neuronal and non-neuronal cell types.

Tyrosine at Position 600 Is a Signal for DVMAT-A Localization to SVs in Vivo—To investigate the potential trafficking role of Tyr^{600} *in vivo*, and its relevance for sorting to SVs, we used the GAL4/UAS system to generate transgenic flies expressing wt and Y600A *dVMAT-A*. In addition, to determine whether other residues (*e.g.* the potential dileucine motif) may be important for DVMAT-A trafficking to SVs *in vivo* we generated transgenic lines expressing the Δ2 and Δ3 *dVMAT-A* deletions. Similar to our *in vitro* constructs, the transgenes were HA-tagged to allow us to distinguish them from endogenous DVMAT-A.

We first determined whether any of the DVMAT-A mutants would show defects in trafficking through the secretory pathway and sorting to the nerve terminal. For these experiments, we used the *dVGLUT-GAL4* driver, which includes expression at the larval neuromuscular junction, a convenient preparation for examining synaptic trafficking (38). We find that DVMAT-A Δ3, Δ2, and Y600A all localized to Type I boutons similar to DVMAT-A wt (data not shown). To measure total protein expression we used the pan-neuronal *elav-GAL4* driver to express wild-type and mutant DVMAT-A. Western blot analysis (Fig. 6, *A* and *B*, $n = 3$ per genotype) confirmed that expression of wild-type and mutant DVMAT-A lines was similar in the lines we used for further analysis.

To determine whether Y600A, Δ3, and/or Δ2 would cause a decrease in the localization of DVMAT-A to SVs, we used glycerol velocity gradient fractionation assays (22, 26, 32). Glycerol velocity gradients were performed on *dVMAT-A* wt, Δ3, Δ2, and Y600A mutants expressed using the *elav-GAL4* driver (see "Experimental Procedures" for detailed genotypes and Fig. 6, *A* and *B*, for total expression levels). As shown in Fig. 6*C*, most (88%) of DVMAT-A wt localized to SVs. In contrast, we found that only 16% of DVMAT-A Y600A was found in fractions containing the SV marker DCSP (Fig. 6, *C* and *D*, one-way ANOVA, $p = 0.0009$; *two asterisks*, Bonferroni post test, $p < 0.01$, see "Experimental Procedures" for quantification method). The Δ2 and Δ3 mutants also localized to SV fractions markedly less than DVMAT-A wt (Fig. 6, *C* and *D*; *two asterisks*, Bonferroni post test, $p < 0.01$.). Together, these data indicate that Tyr^{600} is a major signal in the C terminus for localizing DVMAT-A to SVs *in vivo*. However, at present, we cannot rule out subtle differences between the mutants or the possibility that additional motifs contribute to DVMAT trafficking to SVs (see "Discussion").

Deletion of the DVGLUT C Terminus May Slightly Reduce Internalization—VGLUTs are structurally distinct from VMAT and VAChT, and mammalian VGLUTs contain an overlapping but distinct set of potential trafficking motifs (19–21). Similar to VMAT2 and VAChT, all identified signals are in the VGLUT1 C terminus (19–21). Encouraged by our results on DVMAT-A, we next sought to identify endocytosis motifs in DVGLUT and determine how they might affect its localization to synaptic vesicles.

We initially generated a series of truncation mutants in which we deleted varying portions of the C terminus of DVGLUT. All constructs were *myc*-tagged in the large luminal

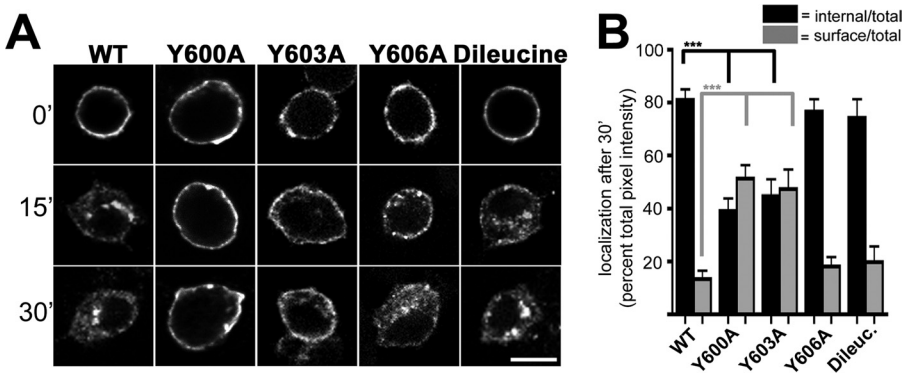

FIGURE 3. **Endocytosis of DVMAT-A point mutants in S2 cells.** *A*, endocytosis assays were performed as in Fig. 2. DVMAT-A wt, Y606A, and dileucine mutant (LI589/590AA) constructs were largely internalized following 30-min incubation, whereas both the Y600A and Y603A constructs remained mostly on the cell surface. *Scale bar*, 5 μm. *B*, quantitation of pixel intensity at the 30-min time point as in Fig. 2 shows that, for DVMAT-A wt, 81 $\pm$ 4% internalized (*black columns*, mean $\pm$ S.D., $\geq$35 cells, from $\geq$3 separate experiments for each genotype). Similarly, 76.6 $\pm$ 4.7% of DVMAT-A Y606A and 74.3 $\pm$ 7% of the dileucine mutant internalized. In contrast, only 39.1 $\pm$ 4.8% of DVMAT-A Y600A and 44.7 $\pm$ 6.4% of DVMAT-A Y603A internalized. One-way ANOVA, $p < 0.0001$; Bonferroni post test, $p < 0.001$ (*black asterisks*) between internal wt and internal Y600A and Y603A. Bonferroni post test, $p < 0.001$ (*gray asterisks*), between cell surface wt and cell surface Y600A and Y603A.

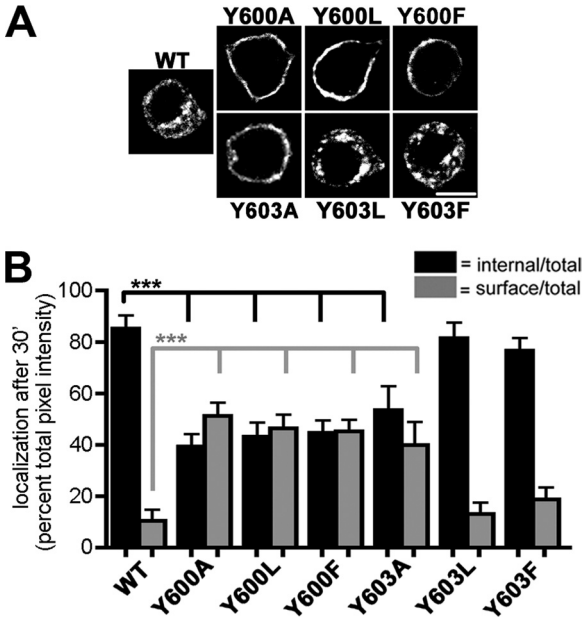

FIGURE 4. **Endocytosis of DVMAT-A bulky group point mutants in S2 cells.** *A*, endocytosis assays were performed as in Fig. 2. DVMAT-A wt, Y603L, and Y603F constructs largely internalized following 30-min incubation, whereas DVMAT-A Y600A, Y600L, Y600F, and Y603A constructs remained mostly on the cell surface. *Scale bar*, 5 μm. *B*, quantitation of pixel intensity at the 30-min time point as in Fig. 2 shows that 85.3 $\pm$ 5% of DVMAT-A wt internalized (*black columns*; mean $\pm$ S.D., $\geq$31 cells from $\geq$3 separate experiments for each genotype). In contrast, only 39.4 $\pm$ 4.8% of DVMAT-A Y600A internalized. Similarly, DVMAT-A Y600L and Y600F showed 43.2 $\pm$ 5.5% and 44.7 $\pm$ 4.9% internalization, respectively. Similar to wt, but in contrast to Y603A, which showed 53.5 $\pm$ 9.3% internalization, 81.5 $\pm$ 6.1% of Y603L and 76.7 $\pm$ 4.9% of Y603F internalized from the cell surface. One-way ANOVA, $p < 0.0001$; Bonferroni post test, $p < 0.001$ (*black asterisks*), between internal wt and internal Y600A, Y603A, Y600F, and Y600L. Bonferroni post test, $p < 0.001$ (*gray asterisks*) between cell surface wt and cell surface Y600A, Y603A, Y600L, and Y600F.

loop of DVGLUT; tagged constructs were expressed at levels similar to the untagged wild-type protein (data not shown). Both N- and C-terminal deletion constructs were able to traffic through the secretory pathway and could be readily detected at the cell surface (Fig. 7*A*, and data not shown). We next tested the effects of these deletions on DVGLUT endocytosis in transfected S2 cells (Fig. 7*B*). Deletion of the C terminus had a small but consistent effect in reducing internalization: as seen at 5 and 15 min, the ring-like labeling of DVGLUT at the cell surface appears more prominent for the C-terminal deletion mutant. At the 30-min time point, however, internalization efficiency was indistinguishable between wt and the C terminus deletion. Moreover, we found it difficult to quantitate the qualitative differences we observed at the 5- and 15-min time points. These observations suggest that the C terminus of DVGLUT is not as important for endocytosis as the C terminus of DVMAT-A and recapitulate previous observations of their mammalian orthologs (see "Discussion").

To determine if the N terminus of DVGLUT might contain additional trafficking signals, we performed a similar set of experiments using an N-terminal deletion. Although we cannot rule out subtle defects in other trafficking events, we did not detect a defect in internalization for the DVGLUT N-terminal deletion (Fig. 7*B*) or in a deletion mutant lacking both the N and C termini (data not shown).

Screening of Potential Trafficking Motifs in DVGLUT—As compared with DVMAT-A, the possible trafficking defects we observed in DVGLUT mutants were minimal. We therefore used an additional genetic method to identify domains and/or specific residues potentially important for DVGLUT trafficking. Overexpression of DVGLUT wt is larval lethal as a result of increased glutamatergic signaling,[4] and expression of a *GFP-dVGLUT* fusion is also lethal. We took advantage of this phenomenon to screen for DVGLUT trafficking mutants that might suppress lethality (see "Experimental Procedures"). Briefly, males containing the *UAS-GFP-dVGLUT* transgene were mutagenized by feeding methanesulfonic acid ethyl ester and then crossed to virgin females containing *dVGLUT-GAL4*. This cross-invariably results in progeny that die as late pupae. We therefore collected suppressors that emerged as adults. Sequencing the *UAS-GFP-dVGLUT* transgene in these suppressors showed that most were intragenic, including 43 lines containing a mutation within the coding region of *dVGLUT* and 3 in the *GFP* moiety fused to the *dVGLUT* N terminus (Table 1). Eight additional mutations did not show a mutation in either *dVGLUT* or *GFP* and are indicated as "wt" in Table 1. Some of these may be second site suppressor mutations, whose positions remain to be mapped.

Many of the suppressor lines showed a complete loss or reduced protein expression. However, several showed a decreased localization to the nerve terminal as compared with

[4] R. Daniels and A. DiAntonio, manuscript in preparation.

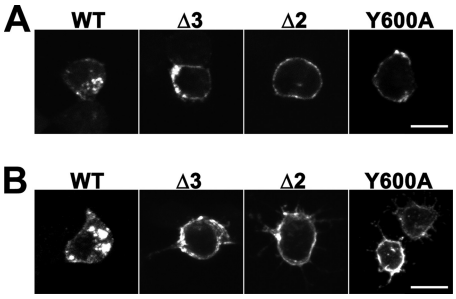

FIGURE 5. **Endocytosis of wt and mutant DVMAT-A constructs in *Drosophila* DmBG2C6 cells.** Endocytosis assays using *Drosophila* DmBG2C6 cells were performed as for S2 cells. DVMAT-A wt was largely internalized following 30-min incubation, whereas DVMAT-A Δ3, Δ2, and Y600A constructs remained mostly on the cell surface as shown in individual optical slices (*A*) and projections (*B*) of confocal images. *Scale bars*, 5 μm.

wild-type DVGLUT (data not shown). These included the stock indicated in Table 1 as B29. Line B29 contains a missense mutation ($Ser^{311} \rightarrow Phe$) in a region of *dVGLUT* that we have shown encodes an intracellular loop between transmembranes 4 and 5 (29). To explore the potential function of this region we generated a series of additional missense and deletion mutations in this cytosolic loop (data not shown). These as well as the original $Ser^{311} \rightarrow Phe$ mutation were expressed in S2 cells followed by immunolabeling as described for the DVGLUT N- and C-terminal deletions. None of the cytosolic loop mutants appeared to reach the cell surface, suggesting that they were trapped in either the endoplasmic reticulum or Golgi (data not shown). It is possible that this region is involved in early trafficking steps, but we also cannot rule out the possibility of a gross structural defect causing retention at an early step in the secretory pathway. Regardless, the inability of the cytosolic loop mutants to reach the cell surface in either S2 cells or at the neuromuscular junction hampered further experiments to determine their potential relevance for either endocytosis or sorting to SVs.

Two other suppressor lines showed enhanced localization to the cell soma as compared with the nerve terminal: B46 (S420F) and B51 (data not shown). Similar to B29 ($Ser^{311} \rightarrow Phe$), we believe that B46 may trap DVGLUT at an early step in the secretory pathway. B51 did not reveal any apparent sequence deviations from wild-type *dVGLUT* and may contain a mutation in a gene other than *dVGLUT*, thus representing a potential second site suppressor as noted above.

Several missense mutations functionally truncated the DVGLUT C terminus, including the line B3 (W530→Stop) that deleted most of the cytoplasmic tail distal to the last transmembrane domain (Fig. 1*B*). As described above, we had previously tested C-terminal deletions generated with *in vitro* mutagenesis, including a $Trp^{530} \rightarrow$ Stop mutant. All were able to reach the surface, and the $Trp^{530} \rightarrow$ Stop mutant may slightly reduce endocytosis. We therefore used the same mutation to determine how the loss of the C terminus would affect sorting of DVGLUT to SVs and refer below to line B3 as *UAS-GFP-dVGLUT-ΔC*.

Deletion of the C Terminus of DVGLUT in Vivo Has a Subtle Effect on Localization to SVs—As described for DVMAT-A, we performed glycerol gradient fractionation on homogenates derived from flies expressing *GFP-dVGLUT-ΔC* as well as endogenous *dVGLUT* (Fig. 8, *A* and *B*). When adjusted for reduced protein expression levels, the mutant localized to SVs ~80% of endogenous DVGLUT levels (Fig. 8*B*). This difference was statistically significant (Student's *t* two tailed, $p = 0.03$) but relatively small compared with the effects of DVMAT-A mutants. The lack of a more robust effect was surprising in light of both the dramatic effects we observed for DVMAT-A C terminus as well as a recent report that demonstrated the importance of the mammalian VGLUT1 C terminus for endocytosis in cultured neurons (19). However, this study on VGLUT1 (19) used a relatively sensitive assay, and endocytosis defects were not observed by groups using other, more standard methods (see "Discussion"). We therefore performed additional experiments in an attempt to sensitize our ability to detect DVGLUT trafficking defects. We reasoned that DVGLUT trafficking defects might be more easily detected as a change in the rate of return to SVs following endocytosis. We used a temperature-sensitive mutation in *Drosophila* dynamin (shi^{ts1}) to force most of the endogenous wt DVGLUT protein to the plasma membrane and thus allow us to track its sorting to SVs after endocytosis. Similar to previously described experiments using other SV proteins (32), we find that exposure of (shi^{ts1}) mutants to a non-permissive temperature to block endocytosis (30 °C) decreased the localization of endogenous wt DVGLUT to SVs. The return of the flies to a permissive temperature (22 °C) for 12 min restored the SV localization of DVGLUT (Fig. 8*C*, *bottom panel*) to steady-state levels.

To test the potential effects of the DVGLUT C-terminal deletions, we recombined the *dVGLUT-GAL4 driver* on the X chromosome with the shi^{ts1} mutation to generate the line *w, shi^{ts1}, dVGLUT-GAL4; UAS-GFP-dVGLUT-ΔC*. We then performed glycerol gradient fractionation experiments as for endogenous DVGLUT in wt flies, but with an extended time course, flash freezing the flies at 0, 1, 4, 7, and 12 min after their return to the permissive temperature. Wild-type DVGLUT from the same homogenates was probed in parallel. The time course in which DVGLUT wt and the DVGLUT ΔC mutant returned to SVs was very similar (Fig. 8*D*), with quantitation showing a minimal reduction for ΔC at each time point (Fig. 8*E*). These data reinforce the idea that the C terminus of DVGLUT may be less important for its localization to SVs than the C terminus of DVMAT-A.

DISCUSSION

We have investigated how potential trafficking domains in two structurally distinct vesicular transporters contribute to endocytosis *in vitro* and their localization to synaptic vesicles *in vivo*. We report that a tyrosine residue in the C terminus of DVMAT-A (Tyr^{600}) is required for efficient internalization in S2 cells and in the *Drosophila* neuronal cell line DmBG2C6. *In vitro* assays further show that the second, but not the first Tyr in $^{600}YXXY^{603}$ can be replaced by phenylalanine or leucine, suggesting that YXXY may be a variant of the YXXΦ motif. Alternatively, YXXY could represent a novel trafficking motif, possibly related to a YXYY motif previously identified in rat VAChT (39). Interestingly, the YXYY motif in VAChT has been reported to bind to the α subunit of AP2 (adaptor protein complex 2) (39) rather than the μ subunit, which binds to the well defined YXXΦ sequence (34). Further work will be needed to

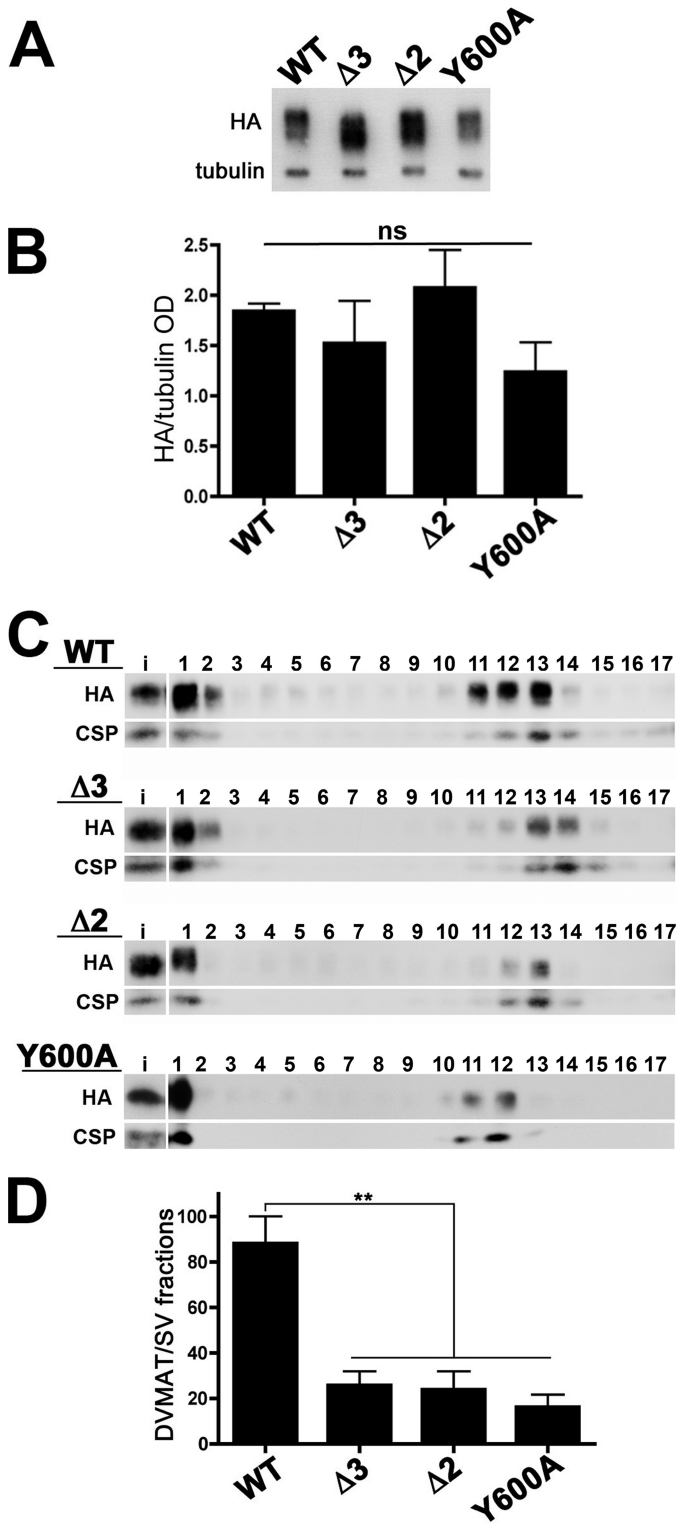

FIGURE 6. **Glycerol velocity gradients of fly heads expressing DVMAT-A.** *A*, comparison of fly lines expressing DVMAT-A wt, Y600A, Δ3, and Δ2 pan-neuronally using an *elav-GAL4* driver (see "Experimental Procedures" for details of genotypes). Homogenates from each genotype were probed on Western blots using mAbs to HA.11 (*top panel*) and the *Drosophila* tubulin protein (*bottom panel*). *B*, three Western blots per genotype (*panel A* and data not shown, mean ± S.E.) were quantified and normalized to the tubulin loading controls. Expression of wt and mutant DVMAT-As is not statistically different ("*ns*"). *C*, the postnuclear homogenates from fly heads expressing DVMAT-A wt, Y600A, Δ3, or Δ2 were separated by glycerol velocity gradient centrifugation, and fractions were probed by Western blots (*fraction #1* is the bottom of the gradient; *fraction #17* is the top of the gradient). The mAb to the HA tag shows the position of DVMAT-A (*top panel* of immunoblots in *C*). DCSP (*bottom panel* of immunoblots in *C*) serves as a marker for SV fractions. A 1:10 dilution of the homogenate loaded onto the gradient (input or "*i*" here and in the text) was probed in parallel. The amounts of HA-tagged DVMAT-A and DCSP were expressed as a percentage of total input loaded onto the gradient (see "Experimental Procedures" for equations). Representative blots show that DVMAT-A wt sedimented in SV fractions to a greater extent than Δ3, Δ2 or Y600A. *D*, quantitation of immunoblots ($n = 3$ for each genotype, mean ± S.E.) shows that DVMAT-A wt was mostly found in synaptic vesicle fractions, and that the localization of DVMAT-A Y600A, Δ3, and Δ2 to synaptic vesicle fractions was reduced relative to wt. One-way ANOVA, $p = 0.0009$. **, Bonferroni post test, $p < 0.01$, for wt control *versus* each of the mutants.

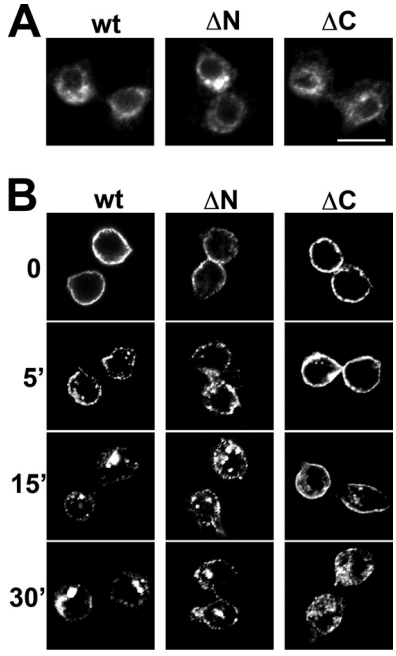

FIGURE 7. **Endocytosis of DVGLUT in S2 cells.** S2 cells expressing DVGLUT wt and deletions of the N (ΔN) and C(ΔC) terminus. *A*, the steady-state expression of each construct was similar. *B*, internalization assays performed as described for DVMAT-A show that ΔN did not appear to differ from wt, whereas ΔC may show a slight reduction in internalization relative to wt at 5 and 15 min, but not at 30 min.

better characterize the Y*XXY* motif in DVMAT-A, and its relationship to Y*XX*Φ; here we have concentrated on its potential role in sorting DVMAT-A to SVs.

dVMAT-A transgenes containing the Y600A mutation show a decreased localization to SVs *in vivo*. Larger deletions of the C terminus do not appear to decrease the localization of DVMAT-A to SVs, indicating that the Y*XXY* motif is a major signal in this domain for localizing DVMAT-A to SVs. It is possible, however, that the techniques we have used were not sensitive enough to detect subtle differences between Y600A and larger deletions. Therefore, at present we cannot rule out the possibility that additional motifs may contribute to the localization of DVMAT-A to SVs. This caveat aside, our data are the first to show that a trafficking motif in a vesicular protein contributes to its localization to SVs *in vivo*.

Our *in vitro* data support a role for Y*XXY* in endocytosis, and we therefore suspect it performs a similar role in sorting DVMAT-A to SVs *in vivo*. A similar motif in rat VAChT (*YXYY*) may function as an endocytosis motif *in vitro* (17) (however, see Ref. 16). At present, we cannot rule out additional roles for Y*XXY* in DVMAT-A, and it remains possible that this

TABLE 1

DVGLUT suppressor mutations

Columns show the designation for each suppressor line ("Line"), the position of mutated residue in wt DVGLUT or GFP ("Site") and the nature of the mutation. Lines that did not appear to contain a mutation in either DVGLUT or GFP are designated "wt" under "Mutation."

	Line	Site	Mutation		Line	Site	Mutation
1	B2	Lys^{9}	Stop	28	B15	Ala^{456}	V
2	B23	Val^{104}	G	29	B13	Gly^{461}	S
3	B34	Gly^{105}	E	30	B9	Gly^{465}	R
4	B4	Asp^{142}	V	31	B44	Ala^{470}	V
5	B39	Gln^{153}	Stop	32	B27	Ala^{497}	V
6	B49	Gln^{153}	Stop	33	RD16	Ala^{497}	V
7	B42	Gly^{157}	D	34	B32	Ser^{513}	F
8	B18	Gly^{203}	E	35	B33	Ser^{513}	F
9	B21	Glu^{206}	K	36	B52	Ser^{513}	F
10	B25	Arg^{220}	Stop	37	B38	Gln^{517}	Stop
11	B22	Gly^{244}	R	38	B16	Trp^{519}	Stop
12	B40	Gly^{244}	R	39	B3	Trp^{530}	Stop
13	B11	Gln^{258}	Stop	40	B45	Trp^{530}	Stop
14	B30	Gly^{265}	R	41	B20	Gln^{613}	Stop
15	B29	Ser^{311}	F	42	B26	Gln^{613}	Stop
16	B28	Trp^{317}	Stop	43	B41	Δ208–252	Deletion
17	B47	Arg^{336}	C	44	B6	–	(wt)
18	B5	Ser^{337}	T	45	B8	–	(wt)
19	B7	Val^{344}	E	46	B10	(GFP)	Stop
20	B19	Gly^{380}	D	47	B12	–	(wt)
21	B48	Ala^{418}	T	48	B14	–	(wt)
22	B46	Ser^{420}	F	49	B17	–	(wt)
23	B24	Thr^{422}	M	50	B31	(GFP)	Stop
24	B43	Thr^{422}	A	51	B35	(GFP)	Stop
25	B50	Val^{433}	E	52	B36	–	(wt)
26	RD7	Gly^{433}	D	53	B37	–	(wt)
27	B1	Pro^{453}	S	54	B51	–	(wt)

motif could mediate sorting of DVMAT-A to other organelles or perhaps recycling to the plasma membrane. Indeed, it is formally possible that some of the DVMAT-A signal scored as cell surface in our *in vitro* assays actually represented protein trapped in early endosomes just below the cell surface. This ambiguity makes it difficult to completely rule out an additional role for Y*XX*Y in trafficking DVMAT-A away from early endosomes and/or recycling to the plasma membrane. Acid-stripping of externally bound antibody and perhaps fluorescence-activated cell sorting would help address this issue, but in our hands, S2 cells are not amenable to either technique (data not shown). Additional experiments using other techniques (*e.g.* DVMAT-A pHluorin constructs similar to those used for VGLUT1 (19)) may help to clarify whether Y*XX*Y could play a role in recycling in addition to internalization.

In contrast to DVMAT-A, we find that potential trafficking motifs within the C terminus of DVGLUT play a much more limited role in internalization in S2 cells and the baseline localization to SVs *in vivo*. As we discuss below, these differences suggest that the pathways that sort VMATs and VGLUTs to SVs at the synapse might also differ.

During SV biogenesis, constitutive secretory vesicles exit via the *trans*-Golgi network and traffic to the plasma membrane for assembly into mature synaptic vesicles (1, 2). To complete SV maturation, vesicles are thought to undergo an endocytosis step at the plasma membrane. In addition, endocytosis of SVs from the plasma membrane is required for SV recycling (3). Because all vesicular proteins must undergo endocytosis during SV biogenesis and recycling, the signals that mediate this trafficking step are thought to be crucial for the localization and function of vesicular transporters. However, all other studies to date have been performed *in vitro* using cultured cells and thus are subject to important limitations. For example, neuroendocrine cell lines such as PC12 cells contain SLMVs rather than SVs, may employ different mechanisms of secretory vesicle biogenesis, and do not make synaptic connections. Primary neuronal cultures circumvent these problems, but are difficult to obtain in large quantities, thus prohibiting most biochemical assays, including those used here to quantitate the localization of DVMAT-A and DVGLUT to SVs.

These limitations aside, previous *in vitro* studies have clearly demonstrated the importance of C-terminal trafficking signals in mammalian vesicular transporters (for a general review of trafficking motifs see Ref. 34). Dileucine motifs in the cytoplasmic C termini of rat VAChT and VMAT2 are necessary for endocytosis in PC12 cells and hippocampal neurons (13, 14) and may be sufficient for sorting to SLMVs in neuroendocrine cells (15, 40). As noted above, mutation of a tyrosine-based motif in the C-terminal trafficking domain of VAChT was shown to cause retention at the plasma membrane in at least one study (17). Mammalian VGLUTs are structurally distinct from both VMATs and VAChT but also have been suggested to use signals in their cytosolic C termini for endocytosis and localization to SVs (19–21). A C-terminal pair of hydrophobic residues in VGLUT1 (FV) has been reported to function similarly to dileucine motifs and to play an important role in recycling VGLUT1 to SVs in primary neuronal cultures (19). Similar motifs may be present in VGLUT2 and -3 (19). An additional polyproline motif (PRPPPP) in the C terminus of VGLUT1, but neither VGLUT2 nor -3, binds endophilin and may work in concert with the putative dileucine-like (FV) motif under some circumstances (19–21). VGLUT1 has also been shown to undergo a second, slower AP3 (adaptor protein complex 3)-dependent endocytic pathway that also allows sorting to SVs (19, 41), but the sorting signals for this pathway are not known.

The modest trafficking defects we observe in DVGLUT mutants lacking the C terminus are consistent with previous studies on mammalian VGLUT1 (see below). Nonetheless, it is possible that the contribution of the DVGLUT C terminus for trafficking to SVs differs from mammalian orthologs. The potential dileucine-like motif in the DVGLUT C terminus (see Fig. 1) does not align precisely with the dileucine-like motifs in other VGLUT orthologs, and the specific endocytosis signals in the C terminus remain unclear. In addition, the polyproline motif in VGLUT1 shown to interact with endophilin (19–21) is not apparent in the C terminus of DVGLUT. It is, therefore, possible that DVGLUT contains trafficking motifs at other sites. The cytosolic loop between transmembranes 4 and 5 in DVGLUT (29) and perhaps other VGLUTs could conceivably contain trafficking motifs required for sorting to SVs. However, mutations in this region trapped DVGLUT at the soma in both S2 cells and *in vivo*, suggesting a more basic secretory or structural role for this region. At present, this limits our ability to investigate an additional role for the large cytosolic loop in DVGLUT for trafficking to SVs. Additional motifs in the N terminus of DVGLUT or mammalian VGLUTs may also be important for trafficking. However, we were unable to detect a defect in internalization for DVGLUT N-terminal deletions,

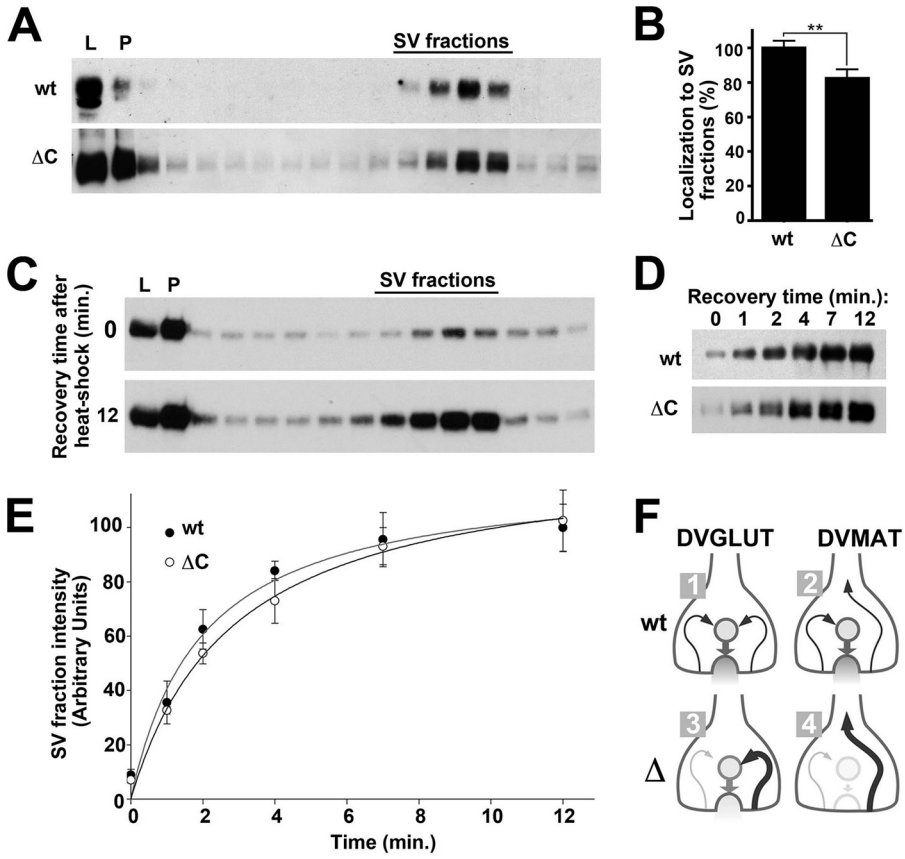

FIGURE 8. **Localization of DVGLUT to SVs *in vivo*.** *A*, steady-state localization. Homogenates from flies expressing the DVGLUT C-terminal deletion mutant were subjected to glycerol velocity gradient fractionation as described for DVMAT-A in Fig. 6. Fractions were probed on Western blots using primary antibodies to endogenous DVGLUT (*wt*, *top*) and to the GFP tag in the ΔC mutant (Δ*C*, *bottom*). *B*, quantitation of three independent experiments shows that the mutant localized to SVs ~80% of wild-type levels. *C*, return of DVGLUT wt to SVs after endocytosis. Flies shifted to the non-permissive temperature for *shi*^{ts1} were assayed immediately (*top panel*, 0 min), or after 12-min recovery at the permissive temperature (*bottom panel*, 12 min). *D*, flies expressing DVGLUT-ΔC were assayed as in *C*, and the relative amount of protein localizing to SV fractions assayed as in *A* and *C* at the indicated time points. *E*, quantitation of *D* and two additional experiments show that DVGLUT wt and ΔC appeared to return to SVs at similar rates. *F*, model of possible differences between VMAT and VGLUT recycling at the synapse. Our data and previous studies suggest that most if not all trafficking at the synapse returns wt VGLUTs to SVs (*F*, *1*). In contrast, we propose that a portion of VMAT may sort into a separate pathway (*F*, *2*). In consequence, mutation of one or more internalization motifs in VMATs can shunt the protein into this pathway and away from SVs (*F*, *4*). In contrast, because of its access to multiple pathways to SVs, disruption of any single pathway does not prevent the VGLUTs from sorting primarily to SVs (*F*, *3*).

and to our knowledge, similar experiments have not been reported for VGLUT1 or any other mammalian ortholog.

Additional domains and motifs beyond Y*XX*Y may also contribute to the trafficking of DVMAT-A. Importantly, the dileucine pair in mammalian VMAT2 functions as a primary endocytosis motif in cultured cells (13). Although the tyrosine motif in DVMAT-A appears as its primary endocytosis motif *in vitro*, and Tyr^{600} is required for the efficient sorting of DVMAT-A to SVs *in vivo*, it remains possible that the conserved dileucine motif in DVMAT-A plays a role in trafficking that has yet to be determined, such as sorting to large dense core vesicles (LDCVs) or as a secondary signal for sorting to SVs that we have not been able to detect using our current assays.

Despite these differences in the function of specific motifs, trafficking of VMATs appears to be fundamentally similar across species, in that mutations of putative trafficking signals cause easily detectable deficits in endocytosis (13, 14, 33, 40, 42), sorting to SLMVs and, as shown here, in sorting to SVs. In contrast, dramatic mutations in the proposed trafficking domains of VGLUTs described here and previously (19, 20) have relatively subtle effects on endocytosis and in sorting to SVs. Importantly, previous experiments on rat VGLUT1 (19) have shown that trafficking mutations redistribute the transporter from one endocytic pathway to another, but do not decrease the total amount of VGLUT1 that sorts to SVs. Another group reported that deletion of the VGLUT1 C terminus had minimal effects on endocytosis (20).

Why might VMAT be more sensitive than VGLUT to the deletion of proposed trafficking signals or domains? It may be significant that VGLUTs belong to a larger family, including transporters that localize to the plasma membrane and lysosomes (12, 43–45). VGLUTs also sort to SLMVs and SVs via an AP3-dependent pathway (19, 46); because VMATs are unable to sort to SLMVs in PC12 cells (47, 48), it is possible that VMATs, unlike VGLUTs, cannot access the AP3-dependent pathway. In addition, VMATs but not VGLUTs sort to LDCVs, a distinct type of secretory vesicle required for peptide release and neuromodulation. For *de novo* biosynthesis, sorting of VMAT2 into LDCVs occurs at the *trans*-Golgi network and requires acidic residues coupled to the dileucine motif as well as a distal acidic patch (14, 33, 42). The fate of VMAT2 following fusion of LDCVs to the plasma membrane remains obscure, but might include recycling back to the Golgi for reincorporation into a new LDCV. If so, at least some synaptic VMAT may need to be sorted away from SVs at the nerve terminal.

One potential model to account for the observed differences between DVMAT-A and DVGLUT and perhaps their mammalian orthologs is shown in *schematic form* in Fig. 8*F*. In this model, endocytosis of VMATs normally sorts them to SVs at the synapse via a single dominant pathway, presumably involving AP2. Mutation of the primary endocytosis signal shunts some protein away from SVs and into an alternative trafficking pathway. In contrast, if VGLUTs can access at least two pathways to SVs, VGLUT trafficking mutants might show more limited defects in sorting to SVs. Consistent with this notion is the observation that all of the recently described VGLUT1 mutants and deletions continued to sort to SVs, switching between AP2 and AP3 pathways depending on which pathway had been blocked (19).

If VMATs and VGLUTs do indeed differ in trafficking at the synapse, how might these differences affect synaptic function and behavior? We suggest that *in vivo* models of vesicular transporter trafficking such as those we report here will be critical to investigate this question.

The similarities between trafficking motifs in mammalian VMATs and DVMAT increase the likelihood that additional information on DVMAT trafficking could be relevant to mechanisms of human disease. Changes in VMAT expression may correlate with some psychiatric illnesses (49–51), and mammalian VMAT2 has been suggested to play a neuroprotective role in both Parkinson disease and stimulant abuse (52, 53). VMAT2 knockout mice show enhanced sensitivity to exogenous neurotoxins as well as the oxidative effects of endogenous dopamine (54–57). Conversely, overexpression of VMAT2 and DVMAT may have neuroprotective effects in mammalian cultured cells (58–61) and in *Drosophila* (62), respectively.

The neuroprotective effects of VMAT2 have been previously proposed to depend on its localization to SVs (63, 64), but the underlying trafficking mechanisms remain unclear. We anticipate that further studies of DVMAT trafficking may help to elucidate this process.

Acknowledgments—We thank Felix Schweizer and Esteban Dell'Angelica for helpful comments on the manuscript, and David E. Patton (deceased) for his contribution to the early phases of the project.

REFERENCES

1. Régnier-Vigouroux, A., Tooze, S. A., and Huttner, W. B. (1991) *EMBO J.* **10,** 3589–3601
2. Hannah, M. J., Schmidt, A. A., and Huttner, W. B. (1999) *Annu. Rev. Cell Dev. Biol.* **15,** 733–798
3. Jahn, R., and Rizzoli, S. O. (2007) *Traffic* **8,** 1121–1122
4. Barbosa, J., Jr., Ferreira, L. T., Martins-Silva, C., Santos, M. S., Torres, G. E., Caron, M. G., Gomez, M. V., Ferguson, S. S., Prado, M. A., and Prado, V. F. (2002) *J. Neurochem.* **82,** 1221–1228
5. Estes, P. S., Roos, J., van der Bliek, A., Kelly, R. B., Krishnan, K. S., and Ramaswami, M. (1996) *J. Neurosci.* **16,** 5443–5456
6. Koenig, J. H., and Ikeda, K. (1989) *J. Neurosci.* **9,** 3844–3860
7. Guichet, A., Wucherpfennig, T., Dudu, V., Etter, S., Wilsch-Bräuniger, M., Hellwig, A., González-Gaitán, M., Huttner, W. B., and Schmidt, A. A. (2002) *EMBO J.* **21,** 1661–1672
8. Fei, H., Grygoruk, A., Brooks, E. S., Chen, A., and Krantz, D. E. (2008) *Traffic* **9,** 1425–1436
9. Eiden, L. E., Schäfer, M. K., Weihe, E., and Schütz, B. (2004) *Pflügers Arch.* **447,** 636–640
10. McIntire, S. L., Reimer, R. J., Schuske, K., Edwards, R. H., and Jorgensen, E. M. (1997) *Nature* **389,** 870–876
11. Sagné, C., El Mestikawy, S., Isambert, M. F., Hamon, M., Henry, J. P., Giros, B., and Gasnier, B. (1997) *FEBS Lett.* **417,** 177–183
12. Reimer, R. J., and Edwards, R. H. (2004) *Pflügers Arch.* **447,** 629–635
13. Tan, P. K., Waites, C., Liu, Y., Krantz, D. E., and Edwards, R. H. (1998) *J. Biol. Chem.* **273,** 17351–17360
14. Li, H., Waites, C. L., Staal, R. G., Dobryy, Y., Park, J., Sulzer, D. L., and Edwards, R. H. (2005) *Neuron* **48,** 619–633
15. Colgan, L., Liu, H., Huang, S. Y., and Liu, Y. J. (2007) *Traffic* **8,** 512–522
16. Ferreira, L. T., Santos, M. S., Kolmakova, N. G., Koenen, J., Barbosa, J., Jr., Gomez, M. V., Guatimosim, C., Zhang, X., Parsons, S. M., Prado, V. F., and Prado, M. A. (2005) *J. Neurochem.* **94,** 957–969
17. Kim, M. H., and Hersh, L. B. (2004) *J. Biol. Chem.* **279,** 12580–12587
18. Varoqui, H., and Erickson, J. D. (1998) *J. Biol. Chem.* **273,** 9094–9098
19. Voglmaier, S. M., Kam, K., Yang, H., Fortin, D. L., Hua, Z., Nicoll, R. A., and Edwards, R. H. (2006) *Neuron* **51,** 71–84
20. Vinatier, J., Herzog, E., Plamont, M. A., Wojcik, S. M., Schmidt, A., Brose, N., Daviet, L., El Mestikawy, S., and Giros, B. (2006) *J. Neurochem.* **97,** 1111–1125
21. De Gois, S., Jeanclos, E., Morris, M., Grewal, S., Varoqui, H., and Erickson, J. D. (2006) *Cell Mol. Neurobiol.* **26,** 679–693
22. Daniels, R. W., Collins, C. A., Gelfand, M. V., Dant, J., Brooks, E. S., Krantz, D. E., and DiAntonio, A. (2004) *J. Neurosci.* **24,** 10466–10474
23. Greer, C. L., Grygoruk, A., Patton, D. E., Ley, B., Romero-Calderón, R., Chang, H. Y., Houshyar, R., Bainton, R. J., Diantonio, A., and Krantz, D. E. (2005) *J. Neurobiol.* **64,** 239–258
24. Daniels, R. W., Gelfand, M. V., Collins, C. A., and DiAntonio, A. (2008) *J. Comp. Neurol.* **508,** 131–152
25. Mahr, A., and Aberle, H. (2006) *Gene Expr. Patterns* **6,** 299–309
26. Chang, H. Y., Grygoruk, A., Brooks, E. S., Ackerson, L. C., Maidment, N. T., Bainton, R. J., and Krantz, D. E. (2006) *Mol. Psychiatry* **11,** 99–113
27. Romero-Calderón, R., Uhlenbrock, G., Borycz, J., Simon, A. F., Grygoruk, A., Yee, S. K., Shyer, A., Ackerson, L. C., Maidment, N. T., Meinertzhagen, I. A., Hovemann, B. T., and Krantz, D. E. (2008) *PLoS Genet.* **4,** e1000245
28. Greenspan, R. (1997) *Fly Pushing: The Theory and Practice of Drosophila Genetics*, pp. 3–16, Cold Spring Harbor Laboratory Press, Plainview, NY
29. Fei, H., Karnezis, T., Reimer, R. J., and Krantz, D. E. (2007) *J. Neurochem.* **101,** 1662–1671
30. Rubin, G. M., and Spradling, A. C. (1982) *Science* **218,** 348–353
31. Zinsmaier, K. E., Hofbauer, A., Heimbeck, G., Pflugfelder, G. O., Buchner, S., and Buchner, E. (1990) *J. Neurogenet.* **7,** 15–29
32. van de Goor, J., Ramaswami, M., and Kelly, R. (1995) *Proc. Natl. Acad. Sci. U.S.A.* **92,** 5739–5743
33. Waites, C. L., Mehta, A., Tan, P. K., Thomas, G., Edwards, R. H., and Krantz, D. E. (2001) *J. Cell Biol.* **152,** 1159–1168
34. Bonifacino, J. S., and Traub, L. M. (2003) *Annu. Rev. Biochem.* **72,** 395–447
35. Boll, W., Ohno, H., Songyang, Z., Rapoport, I., Cantley, L. C., Bonifacino, J. S., and Kirchhausen, T. (1996) *EMBO J.* **15,** 5789–5795
36. Ui-Tei, K., Sakuma, M., Watanabe, Y., Miyake, T., and Miyata, Y. (1995) *Neurosci. Lett.* **195,** 187–190
37. Ui-Tei, K., Nishihara, S., Sakuma, M., Matsuda, K., Miyake, T., and Miyata, Y. (1994) *Neurosci. Lett.* **174,** 85–88
38. Wucherpfennig, T., Wilsch-Bräuninger, M., and González-Gaitán, M. (2003) *J. Cell Biol.* **161,** 609–624
39. Kim, M. H., Lu, M., Kelly, M., and Hersh, L. B. (2000) *J. Biol. Chem.* **275,** 6175–6180
40. Yao, J., and Hersh, L. B. (2007) *J. Neurochem.* **100,** 1387–1396
41. Faúndez, V., Horng, J. T., and Kelly, R. B. (1998) *Cell* **93,** 423–432
42. Krantz, D. E., Waites, C., Oorschot, V., Liu, Y., Wilson, R. I., Tan, P. K., Klumperman, J., and Edwards, R. H. (2000) *J. Cell Biol.* **149,** 379–396
43. Ni, B., Rosteck, P. R., Jr., Nadi, N. S., and Paul, S. M. (1994) *Proc. Natl. Acad. Sci. U.S.A.* **91,** 5607–5611
44. Mancini, G. M., de Jonge, H. R., Galjaard, H., and Verheijen, F. W. (1989) *J. Biol. Chem.* **264,** 15247–15254
45. Butterworth, F. M., Pandey, P., McGowen, R. M., Ali-Sadat, S., and Walia, S. (1995) *Mutat. Res.* **342,** 61–69
46. Salazar, G., Craige, B., Love, R., Kalman, D., and Faundez, V. (2005) *J. Cell Sci.* **118,** 1911–1921
47. Liu, Y., and Edwards, R. H. (1997) *J. Cell Biol.* **139,** 907–916
48. Liu, Y., Schweitzer, E. S., Nirenberg, M. J., Pickel, V. M., Evans, C. J., and Edwards, R. H. (1994) *J. Cell Biol.* **127,** 1419–1433
49. Zubieta, J. K., Huguelet, P., Ohl, L. E., Koeppe, R. A., Kilbourn, M. R., Carr, J. M., Giordani, B. J., and Frey, K. A. (2000) *Am. J. Psychiatry* **157,** 1619–1628
50. Zubieta, J. K., Taylor, S. F., Huguelet, P., Koeppe, R. A., Kilbourn, M. R., and Frey, K. A. (2001) *Biol. Psychiatry* **49,** 110–116
51. Little, K. Y., Krolewski, D. M., Zhang, L., and Cassin, B. J. (2003) *Am. J. Psychiatry* **160,** 47–55
52. Edwards, R. H. (1992) *Curr. Opin. Neurobiol.* **2,** 586–594
53. Fleckenstein, A. E., and Hanson, G. R. (2003) *Eur. J. Pharmacol.* **479,**

283–289
54. Gainetdinov, R. R., Fumagalli, F., Wang, Y. M., Jones, S. R., Levey, A. I., Miller, G. W., and Caron, M. G. (1998) *J. Neurochem.* **70,** 1973–1978
55. Fumagalli, F., Gainetdinov, R. R., Wang, Y. M., Valenzano, K. J., Miller, G. W., and Caron, M. G. (1999) *J. Neurosci.* **19,** 2424–2431
56. Larsen, K. E., Fon, E. A., Hastings, T. G., Edwards, R. H., and Sulzer, D. (2002) *J. Neurosci.* **22,** 8951–8960
57. Caudle, W. M., Richardson, J. R., Wang, M. Z., Taylor, T. N., Guillot, T. S., McCormack, A. L., Colebrooke, R. E., Di Monte, D. A., Emson, P. C., and Miller, G. W. (2007) *J. Neurosci.* **27,** 8138–8148
58. Liu, Y., Peter, D., Roghani, A., Schuldiner, S., Privé, G. G., Eisenberg, D., Brecha, N., and Edwards, R. H. (1992) *Cell* **70,** 539–551
59. Liu, Y., Roghani, A., and Edwards, R. H. (1992) *Proc. Natl. Acad. Sci. U.S.A.* **89,** 9074–9078
60. Chen, C. X., Huang, S. Y., Zhang, L., and Liu, Y. J. (2005) *Neurobiol. Dis.* **19,** 419–426
61. Mosharov, E. V., Larsen, K. E., Kanter, E., Phillips, K. A., Wilson, K., Schmitz, Y., Krantz, D. E., Kobayashi, K., Edwards, R. H., and Sulzer, D. (2009) *Neuron* **62,** 218–229
62. Sang, T. K., Chang, H. Y., Lawless, G. M., Ratnaparkhi, A., Mee, L., Ackerson, L. C., Maidment, N. T., Krantz, D. E., and Jackson, G. R. (2007) *J. Neurosci.* **27,** 981–992
63. Sandoval, V., Riddle, E. L., Hanson, G. R., and Fleckenstein, A. E. (2002) *J. Neurosci.* **22,** 8705–8710
64. Fleckenstein, A. E., Volz, T. J., and Hanson, G. R. (2009) *Neuropharmacology* **56,** Suppl. 1, 133–138